10. Urban Image Classification: Per-pixel Classifiers, Sub-pixel Analysis, Object-based Image Analysis, and Geospatial Methods

Soe W. Myint[1], Victor Mesev[2], Dale Quattrochi[3], and Elizabeth A. Wentz[1]

1 School of Geographical Sciences and Urban Planning, Arizona State University, Coor Hall, 5th floor, 975 S. Myrtle Ave., Tempe, AZ 85287, USA

2 Department of Geography, Florida State University, 323 Bellamy Building, 113 Collegiate Loop, Tallahassee, FL 32306-2190, USA

3 Earth Science Office, NASA Marshall Space Flight Center, Huntsville, AL 35812, USA

*Author to whom correspondence should be addressed: E-Mail: soe.myint@asu.edu

Keywords: urban classification, per-pixel, sub-pixel, object-based, geospatial.

CONTENTS

1.0 Introduction

Remote sensing methods used to generate base maps to analyze the urban environment rely predominantly on digital sensor data from space-borne platforms. This is due in part from new sources of high spatial resolution data covering the globe, a variety of multispectral and multitemporal sources, sophisticated statistical and geospatial methods, and compatibility with GIS data sources and methods. The goal of this chapter is to review the four groups of classification methods for digital sensor data from space-borne platforms; per-pixel, sub-pixel, object-based (spatial-based), and geospatial methods. Per-pixel methods are widely used methods that classify pixels into distinct categories based solely on the spectral and ancillary information within that pixel. They are used for simple calculations of environmental indices (e.g., NDVI) to sophisticated expert systems to assign urban land covers (Stefanov et al., 2001). Researchers recognize however, that even with the smallest pixel size the spectral information within a pixel is really a combination of multiple urban surfaces. Sub-pixel classification methods therefore aim to statistically quantify the mixture of surfaces to improve overall classification accuracy (Myint, 2006a). While within pixel variations exist, there is also significant evidence that groups of nearby pixels have similar spectral information and therefore belong to the same classification category. Object-oriented methods have emerged that group pixels prior to classification based on spectral similarity and spatial proximity. Classification accuracy using object-based methods show significant success and promise for numerous urban

applications (Myint et al., 2011). Like the object-oriented methods that recognize the importance of spatial proximity, geospatial methods for urban mapping also utilize neighboring pixels in the classification process. The primary difference though is that geostatistical methods (e.g., spatial autocorrelation methods) are utilized during both the pre- and post-classification steps (Myint and Mesev, 2012).

Within this chapter, each of the four approaches is described in terms of scale and accuracy classifying urban land use and urban land cover; and for its range of urban applications. We demonstrate the overview of four main classification groups in Figure 1 while Table 1 details the approaches with respect to classification requirements and procedures (e.g., reflectance conversion, steps before training sample selection, training samples, spatial approaches commonly used, classifiers, primary inputs for classification, output structures, number of output layers, and accuracy assessment). The chapter concludes with a brief summary of the methods reviewed and the challenges that remain in developing new classification methods for improving the efficiency and accuracy of mapping urban areas.

Insert Figure 1 here

Insert Table 2

2.0 Remote sensing methods for urban classification and interpretation

Urban areas are comprised of a heterogeneous patchwork of land covers and land uses that are juxtaposed so that classification of specific classes using remote sensing data can be problematic. Derivation of classification methods for urban landscape features has evolved in tandem with

increasing spatial, spectral, and temporal resolutions of remote sensing instruments (e.g., from 90 m Landsat Multispectral Scanner-MSS to 30 m to the Landsat Enhanced Thematic Mapper Plus [ETM+] and Operational Land Imager [OLI] data and progressing to sub-meter spatial resolution products available from commercial systems such as .34 m Geoeye) to achieve more robust digital classification schemes. This evolution of classification techniques, however, does not imply that one method is better than another. As with the type of satellite remote sensing data that are employed for analyses, the application of a specific algorithm for classification of urban land cover and land use is dependent upon what the user's objectives are, and what level of detail, frequency, and sensors are required for the anticipated or resulting output products. Table 2 shows urban remote sensing applications with regards to spatial, temporal, and sensor resolutions.

2.1 Per-pixel methods

Scale is indelible when conducting per pixel classifications. The spatial resolution of the sensor dictates the classification type, range, and accuracy of urban land use and urban land cover. That is because individual urban features are rarely the same size as pixels, nor are they conveniently rectangular in shape. Add temporal scale representing rapid urban activity and per pixel classifications become even more removed from reality. Refining the spatial resolution and reducing the area of the pixel does not necessarily lead to improvements in classification accuracy, and may even introduce additional spectral noise, especially when pixels are smaller than urban features. In all, the ideal situation that each pixel can be identified to represent conclusively one and only one land cover type has now long been abandoned. So too the perfect

relationship between the pixel and the field-of-view, which assumes reflectance is recorded entirely and uniformly from within the spatial limits of individual pixels (Figure 1).

Regardless, the appeal of per-pixel or hard classifications remains; predominantly because they produce crisp and convenient thematic coverages that can be easily integrated with raster-based GIS models (Table 1). Composite models and methodologies containing information from remotely sensed sources are critical for revising databases and for producing comprehensive query-based urban applications. To preserve this relationship with GIS, the quality of per-pixel classifications must be monitored not only using conventional determination of accuracy based on comparisons with more reliable reference data, but also in relation to levels of suitability or 'scale of appropriateness.' Both were evident in the USGS hierarchical scheme (Anderson et al., 1976) using the much-cited 85% as a general guideline for the accuracy of urban features, and which subsequently established a benchmark for researchers to attain and supersede using a variety of statistical and stochastic per-pixel techniques. Some of these focused exclusively on maximizing computational class separability, using the traditional maximum likelihood algorithm (Strahler 1980) and the more recent support vector machines (Yang, 2011), while others developed methodologies that imported extraneous information when aggregating spectrally similar pixels (Mesev, 1998), by incorporating contextual relationships (Stuckens et al., 2000), or by measuring pixel inter-connectivity (Barr and Barnsley, 1997). In both, classification accuracy typically improves only marginally, simply because there is an inherent numerical limitation to the extent individual pixel values can comprehensively represent the multitude of true urban features within the rigid confines of their regular-sized pixel limits (Fisher, 1997).

However within these numerical limits per-pixel classification accuracy can be consistently high if the appropriate spatial resolution (i.e., pixel size) is identified with respect to the suitable level of urban detail (Table 2). Such ideas of scale appropriateness can be traced back to Welch (1982), and have since been widely accepted as an important part of the class training process. But the decision is far from trivial, and must also consider the appropriate scale of analysis (Mesev, 2012). Consider a continuous scale that can be conceptualized by levels of measurement from remote sensor data; ranging from the representation of atomistic urban features (building, tree, sidewalk, etc.) at the micro scale, to the representation of aggregate urban features (residential neighborhoods, industrial zones, or even complete urban areas) at the macro scale. Micro urban remote sensing by per-pixel classification remains highly tenuous (even using meter and sub meter resolutions from the latest sensors) and any reliable interpretation is extracted directly from the spatial orientation of pixels—in a similar vein to conventional interpretation of aerial photography, but with lower clarity and with limited stereoscopic capabilities. However, the spectral heterogeneity problem is less restrictive at the macro scale of analysis where classified pixels, instead of measuring individual urban objects, can be aggregated to represent a generalized view of urban areas, including total imperviousness, approximate lateral growth, and overall greenness. It is at this scale of analysis that many types of urban processes, such as sprawl, congestion, poverty, land use zoning, storm water flow, and heat islands, can be studied simultaneously across an entire urban area as part of the search for theories of livability and sustainability. In sum, per-pixel classifications produce simple and convenient thematic maps of urban land use and land cover that can be incorporated into GIS models. The spatial resolution of the remote sensor, however, limits their accuracy away from mapping individual urban features

with any level of pragmatic precision and towards more traditional macro scales of generalized land cover combinations reminiscent of the timeless V-I-S model (Ridd, 1995).

Insert Table 2 here

2.2 Sub-pixel methods

If locational and thematic accuracy of urban representation from remote sensing is paramount, per-pixel classifications can be modified statistically to measure spectral mixtures representing multiple land cover classes within individual pixels. These are termed sub-pixel algorithms or soft classifications because pixels are no longer constrained to representing single classes, but instead represent various proportions of land cover classes which are conceptually more akin to the spatial and compositional heterogeneity of urban configurations (Ji and Jensen, 1999; Small, 2004). The debate on which approach, per-pixel or sub-pixel, can again be tied to the scale of urban analysis. For example, the measurement of impervious surfaces is particularly amenable to sub-pixel classification because pixels can represent a continuum of imperviousness, from total coverage (downtown areas and industrial estates) to scant dispersion intermingled with bio-physical land covers (city parks). Extensive research has been devoted to more precise quantification of impervious surfaces, and other urban land covers at sub-pixel level, such as linear mixture models (Wu and Murray, 2003; Rashed, et al., 2003), background removal spectral mixture analysis (Ji and Jensen, 1999; Myint, 2006a), Bayesian probabilities (Foody et al., 1992; Mesev, 2001; Eastman and Laney, 2002; Hung and Ridd, 2002), artificial neural network (Foody and Aurora, 1996; Zhang and Foody, 2001), normalized spectral mixture analysis (Wu and Yuan, 2007; Yuan and Bauer, 2007), fuzzy c-means methods (Fisher and

Pathirana, 1990; Foody 2000), multivariate statistical analysis (Bauer *et al*., 2004; Yang and Liu, 2005; Bauer *et al*., 2007), and regression trees (Yang *et al*., 2003a and 2003b; Homer *et al*., 2007).

Among these, linear spectral mixture analysis, regression analysis, and regression trees have had a wider appeal because they are theoretically and computationally simpler, as well as more prevalent in many commercial software packages. However, the success of measuring urban land cover types using linear techniques is dependent on identifying spectrally-pure endmembers, preferably using reference samples collected in the field (Adams et al., 1995; Roberts et al., 1998 and 2012). Although Weng and Hu (2008) derived moderate accuracy levels from employing linear spectral mixture analysis using ASTER and Landsat ETM+ sensor imagery, they discovered that artificial neural networks were also capable of performing non-linear mixing of land cover types at the sub-pixel level (Borel and Gerstl, 1994; Ray and Murray, 1996). Another limitation with linear spectral mixture classifiers is that they do not permit the number of endmembers to be greater than the number of spectral bands (Myint, 2006a). In response, a multiple endmember spectral mixture analysis (MESMA) has been developed to identify many more endmember types to represent the heterogeneous mixture of urban land cover types (Rashed et al., 2003; Powell et al., 2007; Myint and Okin, 2009). Diagrams demonstrating linear spectral mixture analysis and multiple endmember spectral mixture analysis are provided in Figures 2 and 3 respectively.

Figure 2 here

Figure 3 here

Two challenges dominate the research efforts to improve subpixel analysis methods for urban settings. The first challenge is pixel size. Identifying endmembers for all classes in images with large to medium pixels in urban areas is difficult given the heterogeneous nature of urban areas. In small spatial distances (e.g., < 30 m), surfaces rapidly change from impervious, to grass, to building. The smaller pixel size (e.g., 1m or submeter), however, is not always the optimal solution. While pixels may not reflect a mixture of the desired endmembers (e.g., a combination of asphalt and grass), reflectance from unwanted features begin to appear that need to be filtered (e.g., oil surfaces and automobiles in asphalt; chimneys and air conditions on rooftops). The second limitation is that it is almost impossible to identify all possible endmembers in a study area and classification accuracy can be degraded by the potential presence of unknown classes or unidentified classes (e.g., the asphalt and rooftop examples from above). This is because the classifier is based on the assumption that the sum of the fractional proportions of all possible endmembers in a pixel is equal to one. Although this type of modeling is conceptually more representative of urban land cover, from a practical standpoint it nonetheless perpetuates the mixed pixel problem and presents thematic and semantic limitations to urban land classification schemes. In other words, output from sub-pixel analysis produces fractional classes that are more difficult to integrate with GIS data and may even limit their portability for comparisons across space and through time.

2.3 Object-based methods

With the representational limitations of purely spectrally-based per-pixel and sub-pixel classifications it was only a matter of time before the shift to the spatial domain gained

momentum. Even from a purely intuitive standpoint finer resolution (i.e., smaller pixels or large cartographic-scale) imagery exhibit higher levels of detailed features that mimic the heterogeneous nature of urban areas. This greater level of spatial detail invariably also leads to many more uncertain spectral classes–known as noise–which can be true but potentially unwanted urban features such as chimneys or manhole covers. Assuming spectral noise is reduced, images with spatial resolutions ranging from about 0.25 to 5 m have the potential to help identify urban structures necessary to perform many urban applications, including estimation of population based on the number of dwellings of different housing types, residential water use, predicting energy consumption, urban heat island, outdoor water use, solar energy use, and storm water pollution modeling (Jensen and Cowen, 1999).

Conceptually, spatial or object-based approaches are most applicable to high spatial resolution remote sensing data, where objects of interest are larger than the ground resolution element, or pixel. Urban objects may be vegetated features of urban landscapes (e.g., trees, shrubs, golf course) or anthropogenic features (e.g., buildings, pools, sidewalks, roads, canals). With regards to mapping categorical data or identifying land use land cover classes, remotely sensed image analysis started to shift from pixel-based (per-pixel) to object based image analysis (OBIA) or geospatial object based image analysis (GEOBIA) around the year 2000 (Blaschke T., 2010). The object-centered classification prototype starts with the generation of segmented objects at multiple scales (Desclee, et al., 2006; Navulur, 2007; Im et al., 2008; Myint et al., 2008). To demonstrate, Walker and Briggs (2007) employed an object-oriented classification procedure to effectively delineate woody vegetation in an arid urban ecosystem using high spatial resolution true-color aerial photography (without the near infrared band) and achieved an overall accuracy

of 81%. Hermosilla et al. (2012) developed two object-based approaches for automatic building detection and localization using high spatial resolution imagery and LiDAR data. Stow et al (2007) further developed object-based classification by taking advantage of the spatial frequency characteristics of multispectral data, and then measuring the proportions of vegetation, imperviousness, and soil sub-objects to identify residential land use in Accra, Ghana (they documented an overall accuracy of 75%). In another study by Zhaou et el (2008), post-classification change detection based on the object-based analysis of multitemporal high spatial resolution produced even higher accuracies of 92% and 94%; while Myint and Stow (2011) demonstrated the effectiveness of object-based strategies based on decision rules (i.e., membership functions) and nearest neighbor classifiers on high spatial resolution Quickbird multispectral satellite data over the city of Phoenix. These are further supported by Myint et al. (2011) who directly compared the accuracy from object-based classifications (90%) with more traditional spectral-based classifications (68%). The land-cover classes that the authors identified for this particular study include buildings, other impervious surfaces (e.g., roads and parking lots), unmanaged soil, trees/shrubs, grass, swimming pools, and lakes/ponds. The study selected 500 samples points that led to approximately 70 points per class (7 total classes) using a stratified random sampling approach for the accuracy assessment of two different subsets of QuickBird over Phoenix. To be consistent and for precise comparison purposes, they applied the same sample points generated for the output generated by the objectbased classifier as the output produced by the traditional classification technique (i.e., maximum likelihood).

In general, spectrally similar signatures such as dark/gray soil, dark/gray rooftops, dark/gray roads, swimming pools/blue color rooftops, and red soil/red rooftop remain problematic even

with object-based approaches. Furthermore, the most commonly used object-oriented software (Definiens or eCognition) is required to perform a tremendous number of segmentations of objects from all spectral bands using various scale parameters. There is no universally accepted method to determine an optimal level of scale (e.g., object size) to segment objects, and a single scale may not be suitable for all classes. The most feasible approach may be to select the bands for membership functions at the scale that identifies the class with variable options and analyze them heuristically on the display screen. Given that the nearest neighbor classifier and decision rule available in the object-based approach are non-parametric approaches, they are independent of the assumption that data values need to be normally distributed. This is advantageous, because most data are not normally distributed in many real world situations. Another advantage of the object-based approach is that it allows additional selection or modification of new objects (training samples) at iterative stages, until the satisfactory result is obtained. However, the object-based approach has a significant problem when dealing with a remotely sensed data over a fairly large area since computer memory needs to be used extensively to segment tremendous numbers of objects using multispectral bands. This is true even for fine spatial resolution data with fewer bands (e.g., QuickBird) over a small study area when requiring smaller scale parameters (smaller objects). Figure 4 shows segmented images at scale level 25, 50, and 100 using a subset of a QuickBird image over Phoenix. Figure 5 demonstrates how hierarchical image segmentation delineates image objects at various scales.

Figure 4 here

Figure 5 here

2.4 Geospatial methods

Texture plays an important role in the human visual system for pattern recognition and interpretation. For image interpretation, pattern is defined as the overall spatial form of related features, where the repetition of certain forms is a characteristic pattern found in many cultural objects and some natural features. Local variability in remotely sensed data, which is part of texture or pattern analysis, can be characterized by computing the statistics of a group of pixels, e.g., standard deviation, coefficient of variance or autocovariance, or by the analysis of fractal similarities or autocorrelation of spatial relationships. There have been some attempts to improve the spectral analysis of remotely sensed data by using texture transforms in which some measure of variability in digital numbers is estimated within local windows; e.g. the contrast between neighboring pixels (Edwards et al., 1988), standard deviation (Arai, 1993), or local variance (Woodcock and Harward, 1992). One commonly used statistical procedure for interpreting texture uses an image spatial co-occurrence matrix, which is also known as a gray level co-occurrence matrix (GLCM) (Franklin et al., 2000). There are a number of texture measures, which could be applied to spatial co-occurrence matrices for texture analysis (Peddle and Franklin, 1991). For instance, Herold et al. (2003) proposed a method based on using landscape metrics to classify IKONOS sensor images, which in turn is compared to a GLCM. Liu et al. (2006) further contrasted spatial metrics, GLCM, and semi-variograms in terms of urban land use classification.

Lam et al. (1998) demonstrated how fractal dimensions yield quantitative insight into the spatial complexity and information contained in remotely sensed data. Quattrochi et al. (1997) went further and created a software package known as the Image Characterization and Modeling

System (ICAMS) to explore how the fractal dimension is related to surface texture. Fractal dimensions were also analyzed by Emerson et al. (1999) who used the isarithm method and Moran's I and Geary's C spatial autocorrelation measures to observe the differing spatial structure of the smooth and rough surfaces in remotely sensed images. In terms of other geospatial techniques, De Jong and Burrough (1995) and Woodcock et al (1988) implemented variograms to measurements derived from remotely sensed to quantitatively describe urban spatial patterns. Myint and Lam (2005a; 2005b) and Myint et al. (2006) developed a number of lacunarity approaches to characterize urban spatial features with completely different texture appearances that may share the same fractal dimension values. Both studies report that lacunarity can be considered more effective in comparison to fractal approaches for urban mapping.

The geospatial methods described so far may not provide satisfactory accuracies when they are applied to the classification of urban features from fine spatial resolution remotely sensed images. That is mainly because most of them focus primarily on coupling features and objects at a single scale and cannot determine the effective representative value of particular texture features according to their directionality, spatial arrangements, variations, edges, contrasts, and the repetitive nature of object and features. There have been a number of reports in spatial frequency analysis of mathematical transforms, which provide solutions using multi-resolution analysis. Recent developments in spatial/frequency transforms such as the Fourier transform, Wigner distribution, discrete cosine transform, and wavelet transform have all provided sound multi-resolution analytical tools (Bovik et al., 1990; Zhu and Yang, 1998).

Of all transformation approaches, wavelets play the most critical part in texture analysis. Wavelets are part of spatial and frequency based classification approaches, and a local window plays an important role in measuring and characterizing spatial arrangements of objects and features. Homogeneity, size of regions, characteristic scale, directionality, and spatial periodicity are important issues that should be considered to identify local windows when performing wavelet analysis (Myint, 2010). From a computational perspective, the ideal window size is the smallest size that also produces the highest accuracy (Hodgson, 1998). The accuracy should increase with a larger local window size since it contains more information than a smaller window size and therefore provides more complete coverage of spatial variation, directionality and spatial periodicity of a particular texture. However, minimization of local window size is also important in spatial-based urban image classification techniques since a larger window size tends to cover more urban land cover features and consequently creates mixed boundary pixels or mixed land cover problems. However, some spatial and frequency approaches such as wavelet dyadic decomposition approaches require large window sizes to capture spatial information at multiple scales (Myint, 2006b). The potential solution to this problem would be to employ a multi-scale overcomplete wavelet analysis using an infinite scale decomposition procedure. This is because a large spatial coverage or a large local window is not needed to describe a spatial pattern. Furthermore, this approach can measure different directional information of anisotropic features at unlimited scales, and it is designed to normalize and select effective features to identify urban classes. Myint and Mesev (2012) employed a wavelet-based classification method to identify urban land use and land cover classes using different decision rule sets and spatial measures and demonstrated the effectiveness of wavelets. However, the current wavelet-based classification system with the dyadic wavelet approach is limited by the fact that higher-level

sub-images are just a quarter of the preceding image. In general, smaller window size is generally thought to yield higher accuracy in geospatial-based image classification because if the window is too large, much spatial information from two or more land cover classes could create a mixed boundary problem. Further research is required to consider an overcomplete wavelet approach that can generate spatial arrangements of objects and features at any scale level for urban mapping. Such an approach could potentially be applicable to any land use/ land cover system at any resolution or scale because it can effectively use any window size. Figure 6 shows how wavelet approaches work in comparison to other geospatial approaches in urban mapping.

Figure 6 here

3.0 Concluding remarks

Interpreting urban land cover from data captured by remote sensors remains a conceptual and technical challenge. Accuracy levels are typically lower than the interpretation of more naturally-occurring surfaces. However, huge strides have been made with the formulation of statistical models that help disentangle the spectral and spatial complexity of urban land covers. Whereas per-pixel classification have stood the test of time (primarily for pragmatic reasons, especially when integrated with GIS-handled datasets), developments in sub-pixel, object-based and geospatial techniques have begun, at last, to reproduce the geographical configuration and compositional texture of urban structures. These developments are further tempered by conceptual developments that now consider the “appropriateness” of scale (understanding the level of urban structural measurements) and the “appropriateness” of time (understanding the lag between urban process and urban structure). Both are critical for measuring the rate of urban

change; not simply the amount of lateral growth, but also the juxtaposition of land use within existing urban limits. Further research will only improve our use of remote sensor data for measuring urban patterns and in turn will complement our understanding of key urban processes.

4.0 References:

Adams, J. B., Sabol, D. E., Kapos, V., Almeida-Filho, R., Roberts, D. A., Smith, M. O. & Gillespie, A.R. 1995. Classification of multiple images based on fractions of endmembers: application to landcover change in the Brazilian Amazon, Remote Sensing of Environment, 52, 137–154.

Anderson, J. R., Hardy, E. E., Roach, J. T. and Witmer, R. E. 1976. A land use and land cover classification system for use with remote sensor data. U.S. Geological Survey Professional Paper, 964. http://landcover.usgs.gov/pdf/anderson.pdf.

Arai, K., 1993. A classification method with a spatial-spectral variability. International Journal of Remote Sensing, 14, 699-709.

Barr, S., & Barnsley, M. A., 1997. A region-based, graph-theoretic data model for the inference of second-order thematic information from remotely-sensed images. International Journal of Geographical Information Science, 11, 555-576.

Bauer, M. E., Heinert, N. J., Doyle, J. K., & Yuan, F. 2004. Impervious surface mapping and change monitoring using satellite remote sensing, Proceedings of the ASPRS 2004 Annual Conference, 24-28 May, Denver, Colorado.

Bauer, M. E., Loeffelholz, B. C., & Wilson, B. 2007. Estimating and mapping impervious surface area by regression analysis of Landsat imagery. In Q. Wang (Ed.), Remote Sensing of Impervious Surfaces, pp. 3-20. Boca Raton, Florida: CRC Press.

Blaschke T. 2010. Object-based image analysis for remote sensing. ISPRS International Journal of Photogrammetry and Remote Sensing, 65, 2–16.

Borel, C. C., & Gerstl, S. A. W. 1994. Nonlinear spectral mixing models for vegetative and soil surfaces, Remote Sensing of Environment, 47, 403-416.

Bovik, A. C., Clark, M., & Geisler, W. S., 1990. Multichannel texture analysis using localized spatial filters. IEEE Transactions on Pattern Analysis and Machine Intelligence, 12, 55-73.

De Jong, S. M., & Burrough, P. A. 1995. A fractal approach to the classification of Mediterranean vegetation types in remotely sensed images. Photogrammetric Engineering and Remote Sensing, 61, 1041-1053.

Desclée, B., Bogaert, P., & Defourny, P. 2006. Forest change detection by statistical object-based method. Remote Sensing of Environment, 102, 1-11.

Eastman, J. R., Laney, R. M. 2002. Bayesian soft classification for sub-pixel analysis: a critical evaluation. Photogrammetric Engineering and Remote Sensing, 6811, 1149-1154.

Edwards, G., Landry, R., & Thompson, K. P. B. 1988. Texture analysis of forest regeneration sites in high-resolution SAR imagery. Proceedings of the International Geosciences and Remote Sensing Symposium (IGARSS 88), ESA SP-284, pp. 1355-1360. European Space Agency, Paris.

Emerson, C. W., Lam, N. S. N., & Quattrochi, D. A. 1999. Multi-scale fractal analysis of image texture and pattern. Photogrammetric Engineering and Remote Sensing, 65, 51-61.

Fisher, P. 1997. The pixel: a snare and a delusion. International Journal of Remote Sensing, 18, 679-685.

Fisher, P. F., & Pathirana, S., 1990. The evaluation of fuzzy membership of land cover classes in the suburban zone. Remote Sensing of Environment, 34, 121-132.

Foody, G. M., 2000. Estimation of sub-pixel land cover composition in the presence of untrained classes. Computers and Geosciences, 26, 469-478.

Foody, G. M., Campbell, N. A., Trodd, N. M. & Wood, T. F. 1992. Derivation and applications of probabilistic measures of class membership from the maximum-likelihood classification.

Photogrammetric Engineering and Remote Sensing, 58, 1335-1341.

Foody, G. M. & Aurora, M. K. 1996. Incorporating mixed pixels in the training, allocation and testing of supervised classification. Pattern Recognition Letters, 17, 1389-1398.

Franklin, S. E., Hall, R. J., Moskal, L. M., Maudie, A. J. & Lavigne, M. B. 2000. Incorporating texture into classification of forest species composition from airborne multispectral images, International Journal of Remote Sensing, 21, 61-79.

Hermosilla, T., Ruiz, L. A., Recio, J. A., & Cambra-López, M. 2012. Assessing contextual descriptive features for plot-based classification of urban areas, Landscape and Urban Planning, 106, 124–137.

Herold, M., Liu, X. & Clarke, K. C. 2003. Spatial metrics and image texture for mapping urban land use. Photogrammetric Engineering and Remote Sensing, 69, 991-1001.

Hodgson, M. E. 1998. What size window for image classification? A cognitive perspective. Photogrammetric Engineering and Remote Sensing, 64, 797-807.

Homer, C., Dewitz, J., Fry, J., Coan, M., Hossain, N., Larson, C., Herold, N., McKerrow, A., VanDriel, J. N. & Wickham, J. 2007. Completion of the 2001 national land cover database for the conterminous United States. Photogrammetric Engineering & Remote Sensing, 73, 337–341.

Hung, M. & Ridd, M. K. 2002. A subpixel classifier for urban land-cover mapping based on a maximum-likelihood approach and expert system rules. Photogrammetric Engineering and Remote Sensing, 68, 1173-1180.

Im, J., Jensen, J. R., & Hodgson, M. E. 2008. Object-based land cover classification using high posting density lidar data. GIScience and Remote Sensing, 45, 209-228.

Jensen, J. R., & Cowen, D. C. 1999. Remote sensing of urban/suburban infrastructure and socio-economic attributes. Photogrammetric Engineering and Remote Sensing, 65, 611-622.

Ji, M. & Jensen, J. R. 1999. Effectiveness of subpixel analysis in detecting and quantifying urban impervious from Landsat Thematic Mapper Imagery. Geocarto International, 14, 33-41.

Lam, N. S. N, Quattrochi, D., Qui, H. & Zhao, W. 1998. Environmental assessment and monitoring with image characterization and modeling system using multiscale remote sensing data. Applied Geographic Studies, 2, 77-93.

Liu. X., Clarke, K. C., & Herold, M. 2006. Population density and image texture: a comparison study. Photogrammetric Engineering and Remote Sensing, 72, 187-196.

Mesev, V. 1998. The use of census data in urban image classification. Photogrammetric Engineering and Remote Sensing, 64, 431-438.

Mesev, V. 2001. Modified maximum likelihood classifications of urban land use: spatial segmentation of prior probabilities. Geocarto International, 16, 41-48.

Mesev, V. 2012. Multiscale and multitemporal urban remote sensing. ISPRS International Archives of the Photogrammetry, Remote Sensing & Spatial Information Sciences, XXXIX-B2, 17-21.

Myint, S. W. 2006a. Urban vegetation mapping using sub-pixel analysis and expert system rules: A critical approach. International Journal of Remote Sensing, 27, 2645-2665.

Myint, S. W. 2006b. A new framework for effective urban land use land cover classification: A wavelet approach. GIScience and Remote Sensing, 43, 155-178.

Myint, S. W. 2010. Multi-resolution decomposition in relation to characteristic scales and local window sizes using an operational wavelet algorithm. International Journal of Remote Sensing, 31, 2551-2572.

Myint, S. W., Giri, C. P., Wang, L., Zhu, Z., & Gillette, S. 2008. Identifying mangrove species and their surrounding land use and land cover classes using an object oriented approach with a lacunarity spatial measure. GIScience and Remote Sensing, 45, 188-208.

Myint, S. W., Gober, P., Brazel, A., Grossman-Clarke, S., & Weng, Q. 2011. Per-pixel versus object-based classification of urban land cover extraction using high spatial resolution imagery. Remote Sensing of Environment, 115, 1145-1161.

Myint, S. W., & Lam, N. S. N. 2005a. A study of lacunarity-based texture analysis approaches to improve urban image classification. Computers, Environment, and Urban Systems, 29, 501-523.

Myint, S. W., & Lam, N. S. N. 2005b. Examining lacunarity approaches in comparison with fractal and spatial autocorrelation techniques for urban mapping. Photogrammetric Engineering and Remote Sensing, 71, 927-937.

Myint, S. W., & Mesev, V. 2012. A comparative analysis of spatial indices and wavelet-based classification. Remote Sensing Letters, 3, 141–150.

Myint, S. W., Mesev, V., & Lam, N. S. N. 2006. Texture analysis and classification through a modified lacunarity analysis based on differential box counting method. Geographical Analysis, 38, 371-390.

Myint, S. W., & Okin, G. S. 2009. Modelling land-cover types using multiple endmember spectral mixture analysis in a desert city. International Journal of Remote Sensing, 30, 2237–2257.

Myint, S. W., & Stow, D. 2011. An object-oriented pattern recognition approach for urban classification. In X. Yang (Ed.), Urban Remote Sensing, Monitoring, Synthesis and Modeling in the Urban Environment, pp. 129-140. Chichester, UK: John Wiley & Sons, Ltd. doi: 10.1002/9780470979563

Navulur, K. 2007. Multispectral image analysis using the object-oriented paradigm. Boca Raton, Florida: CRC Press, Taylor and Frances Group.

Peddle, D. R., & Franklin, S. E. 1991. Image texture processing and data integration for surface pattern discrimination. Photogrammetric Engineering and Remote Sensing, 57, 413-420.

Powell, R. L., Roberts, D. A., Dennison, P. E., & Hess, L. L. 2007. Sub-pixel mapping of urban land cover using multiple endmember spectral mixture analysis: Manaus, Brazil. Remote Sensing of Environment, 106, 253-267.

Quattrochi, D. A., Lam, N. S. N., Qiu, H., & Zhao, W. 1997. Image characterization and modeling system (ICAMS): A geographic information system for the characterization and modeling of multiscale remote sensing data. In D. A. Quattrochi, & M. F. Goodchild (Eds.), Scale in Remote Sensing and GIS, pp. 295-308. Boca Raton, Florida: CRC Press.

Rashed, T., Weeks, J. R., Roberts, D., Rogan J., & Powell, R. 2003. Measuring the physical composition of urban morphology using multiple endmember spectral mixture models. Photogrammetric Engineering and Remote Sensing, 69, 1011-1020.

Ray, T. W., & Murray, B. C. 1996. Nonlinear spectral mixing in desert vegetation. Remote Sensing of Environment, 55, 59–64.

Ridd, M.K. 1995. Exploring a V-I-S Vegetation-Impervious Surface-Soil model for urban ecosystems analysis through remote sensing: Comparative anatomy for cities. International Journal of Remote Sensing, 16, 2165-2186.

Roberts, D. A., Gardner, M., Church, R., Ustin, S., Scheer, G., & Green, R. O. 1998. Mapping chaparral in the Santa Monica Mountains using multiple endmember spectral mixture models. Remote Sensing of Environment, 65, 267–279.

Roberts, D. A., Quattrochi, D. A., Hulley, G. C., Hook, S. J., & Green, R. O. 2012. Synergies between VSWIR and TIR data for the urban environment: An evaluation of the potential for the hyperspectral Infrared Imager (HyspIRI) decadal survey mission. Remote Sensing of Environment, 117, 83-101.

Small, C. 2004. The Landsat ETM+ spectral mixing space. Remote Sensing of Environment, 93, 1-17.

Stow, D., Lopez, A., Lippitt, C., Hinton, S., & Weeks, J. 2007. Object-based classification of residential land use within Accra, Ghana based on QuickBird satellite data. International Journal of Remote Sensing, 28, 5167-5173.

Stefanov, W. L., Ramsey M. S., & Christensen, P. R. 2001. Monitoring urban land cover change: An expert system approach to land cover classification of semiarid to arid urban centers. *Remote Sensing of Environment* 77(2):173-185.

Strahler, A. H. 1980. The use of prior probabilities in maximum likelihood classification of remotely sensed data. Remote Sensing of Environment, 10, 135-163.

Stuckens, J., Coppin, P. R. & Bauer, M. 2000. Integrating contextual information with per-pixel classification for improved land cover classification. Remote Sensing of Environment, 71, 282-296.

Walker, J. S., & Briggs, J. M. 2007. An object-oriented approach to urban forest mapping with high-resolution, true-color aerial photography. Photogrammetric Engineering & Remote Sensing, 73, 577-583.

Welch, R.A. 1982. Spatial resolution requirements for urban studies, International Journal of Remote Sensing, 3, 139-146.

Weng, Q., & Hu, X. 2008. Medium spatial resolution satellite imagery for estimating and mapping urban impervious surfaces using LSMA and ANN. Transactions on Geoscience and Remote Sensing, 46, 2387-2406.

Woodcock, C., & Harward, V. J. 1992. Nested-hierarchical scene models and image segmentation. International Journal of Remote Sensing, 13, 3167-3187.

Woodcock, C. E, Strahler, A. H., & Jupp, D. L. B. 1988. The use of variograms in remote sensing: I. Scene models and simulated images. Remote Sensing of Environment, 25, 323-348.

Wu, C., & Murray, A. 2003. Estimating impervious surface distribution by spectral mixture analysis. Remote Sensing of Environment, 84, 493-505.

Wu, C., & Yuan, F. 2007. Seasonal sensitivity analysis of impervious surface estimation with satellite imagery. Photogrammetric Engineering & Remote Sensing, 73, 1393–1401.

Yang, L., Huang, C., Homer, C. G., Wylie, B. K., & Coan, M. J. 2003a. An approach for mapping large-area impervious surfaces: Synergistic use of Landsat-7 ETM+ and high spatial resolution imagery. Canadian Journal of Remote Sensing, 29, 230–240.

Yang, L., Xian, G., Klaver, J.M., & Deal, B. 2003b. Urban land-cover change detection through sub-pixel imperviousness mapping using remotely sensed data. Photogrammetric Engineering & Remote Sensing, 69, 1003–1010.

Yang, X. 2011. Parameterizing support vector machines for land cover classification, Photogrammetric Engineering & Remote Sensing, 77, 27-37.

Yang, X., & Liu, Z. 2005. Use of satellite-derived landscape imperviousness index to characterize urban spatial growth. Computers, Environment and Urban Systems, 29, 524-540.

Yuan, F., & Bauer, M. E. 2007. Comparison of impervious surface area and normalized difference vegetation index as indicators of surface urban heat island effects in Landsat imagery. Remote Sensing of Environment, 106, 375–386.

Zhang, J. and Foody, G. M. 2001. Fully-fuzzy supervised classification of sub-urban land cover from remotely sensed imagery: Statistical and neural network approaches. Photogrammetric Engineering and Remote Sensing, 22, 615-628.

Zhou, W. Q., Troy, A. and Grove, M. 2008. Object-based land cover classification and change analysis in the Baltimore metropolitan area using multitemporal high resolution remote sensing data. Sensors, 8, 1613-1636.

Zhu, C., and Yang, X. 1998. Study of remote sensing image texture analysis and classification using wavelet. International Journal of Remote Sensing, 13, 3167-3187.

List of Tables

List of Figures

Note: Sub-images at level two in the dyadic approach reach the suggested minimum dimension (8x8 pixels) since any sub-images smaller than eight pixels may not contain any useful spatial information. A sub-image at a higher level is exactly the same as its original size at the preceding level in the overcomplete approach. It should also be noted that the level of scale with the overcomplete approach is unlimited. A = approximation texture; H = horizontal texture; V = vertical texture; D = diagonal texture.

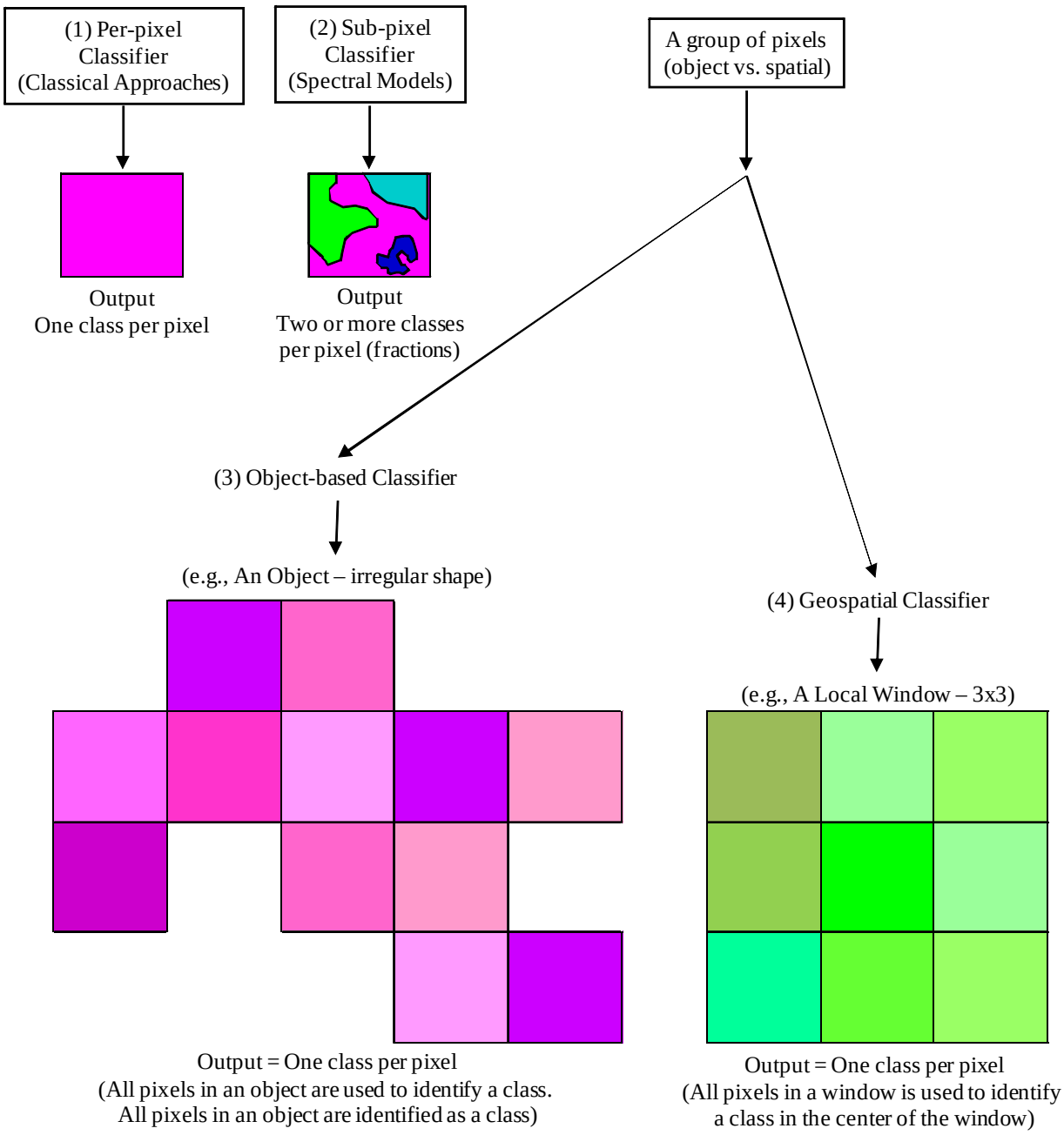

Figure 1. Overview of four main classification groups.

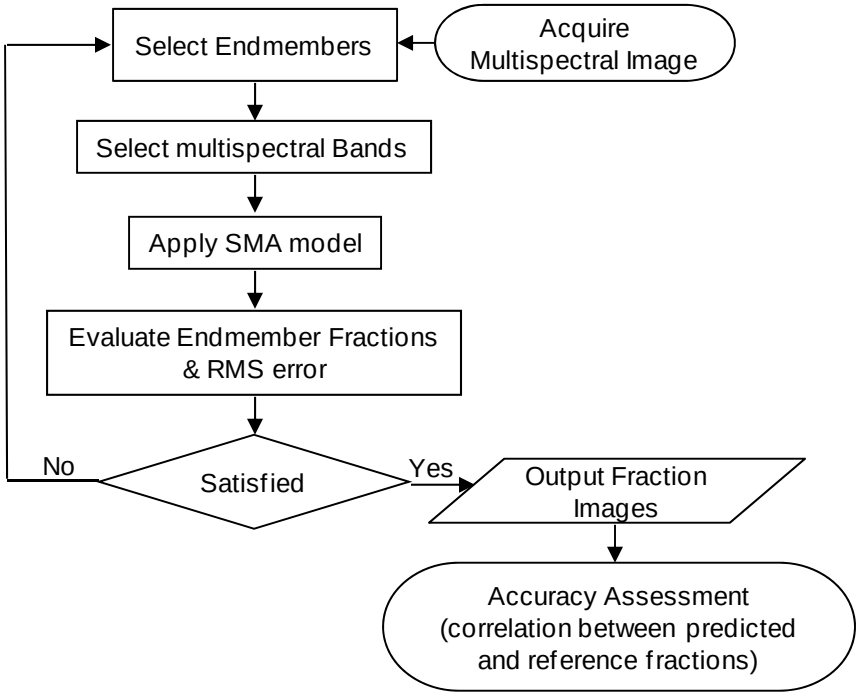

Figure 2. Spectral mixture analysis.

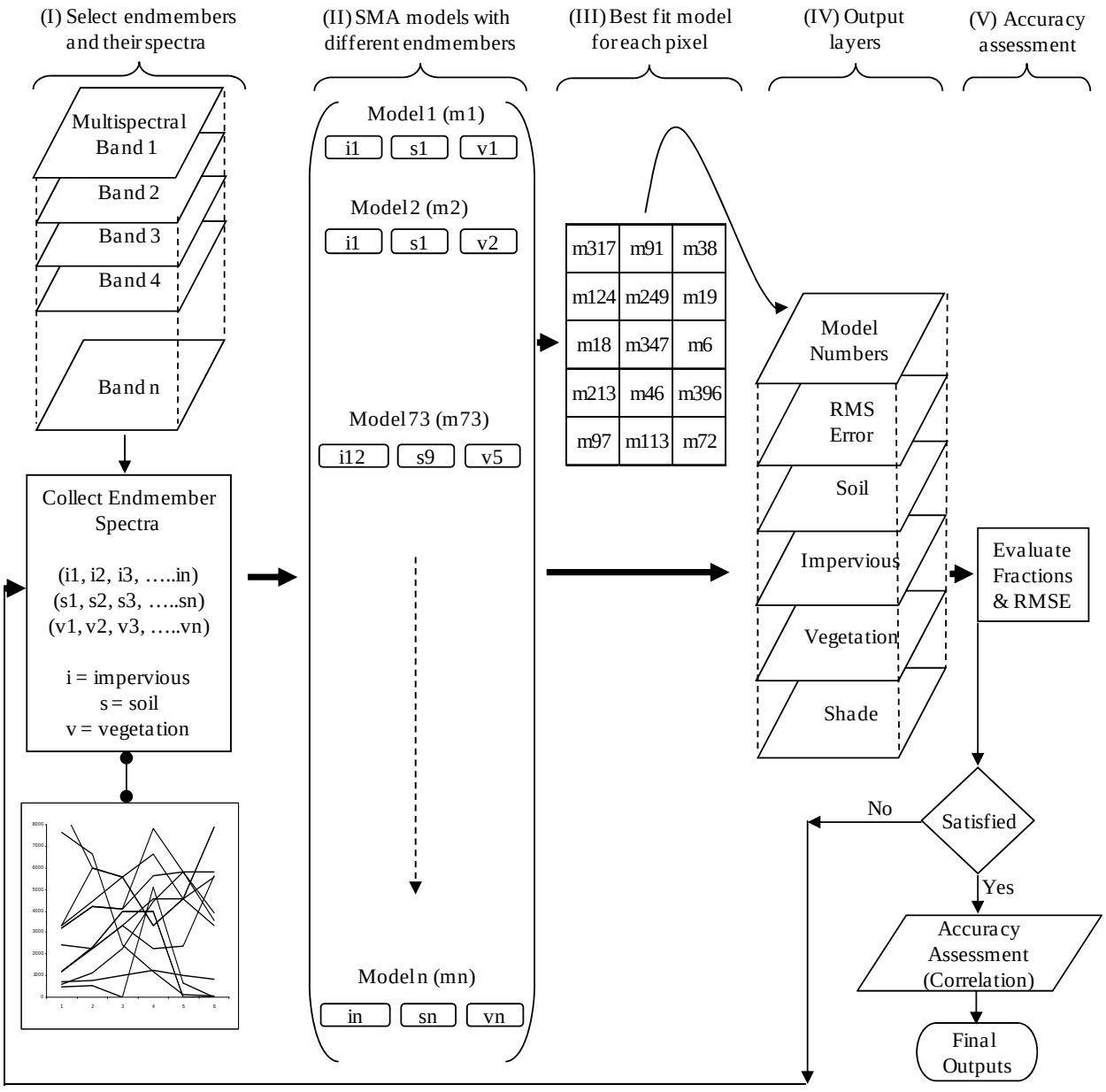

Figure 3. Multiple endmember spectral mixture analysis.

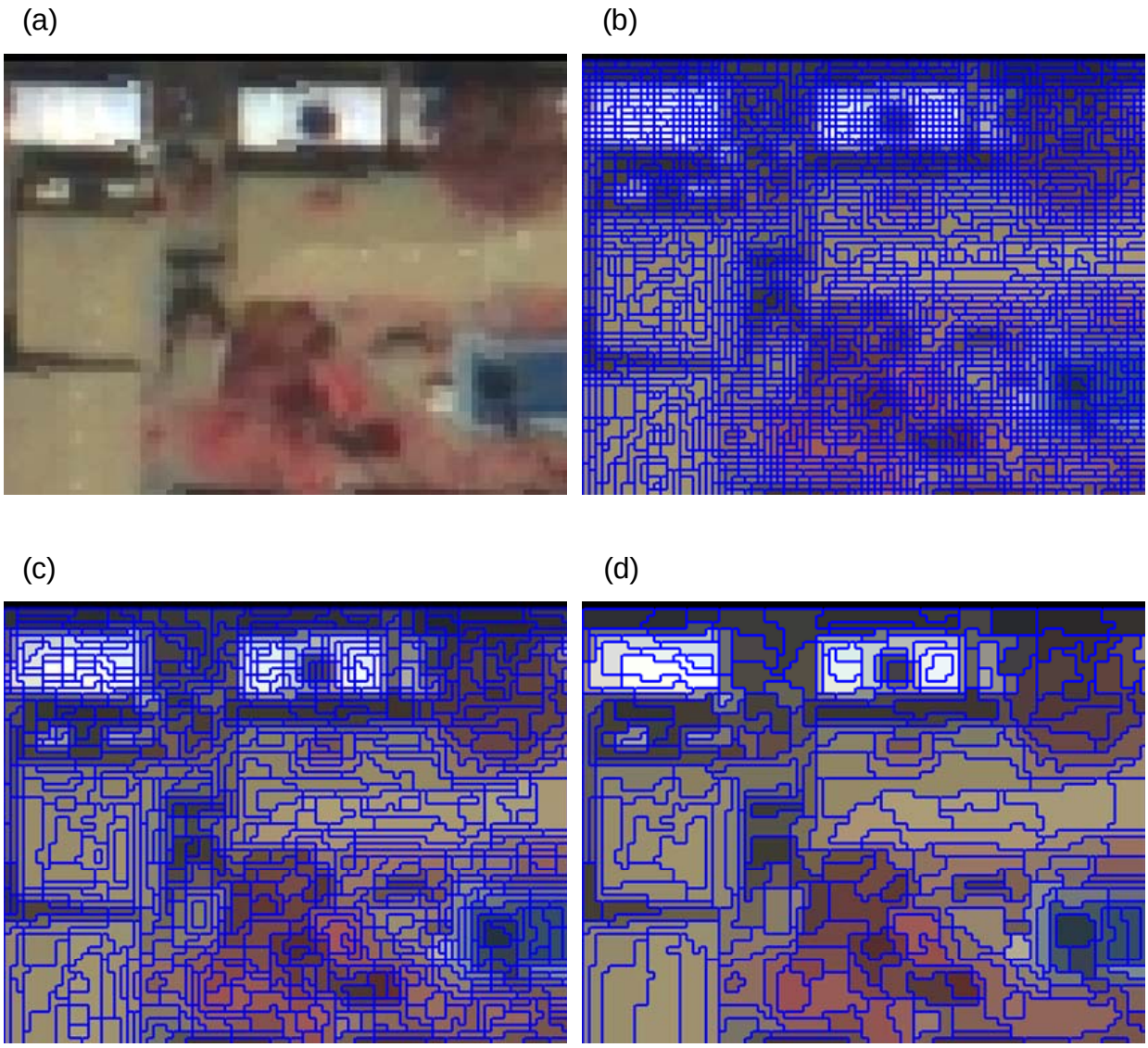

Figure 4. A subset image and segmented images at different scales. (a) Original subset; (b) level 1 (scale parameter 25), (c) level 2 (scale parameters 50), (d) level 3 (scale parameter 100).

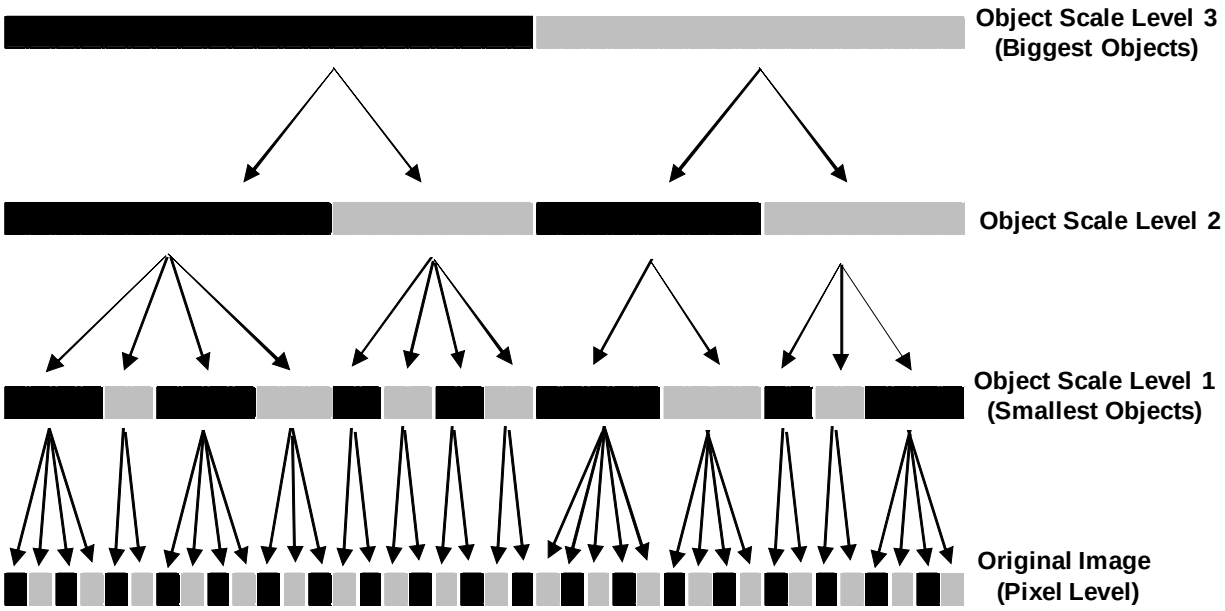

Figure 5. Image objects at each image scale level. Level 3 = 100, level 2 = 50, level 1 = 25.

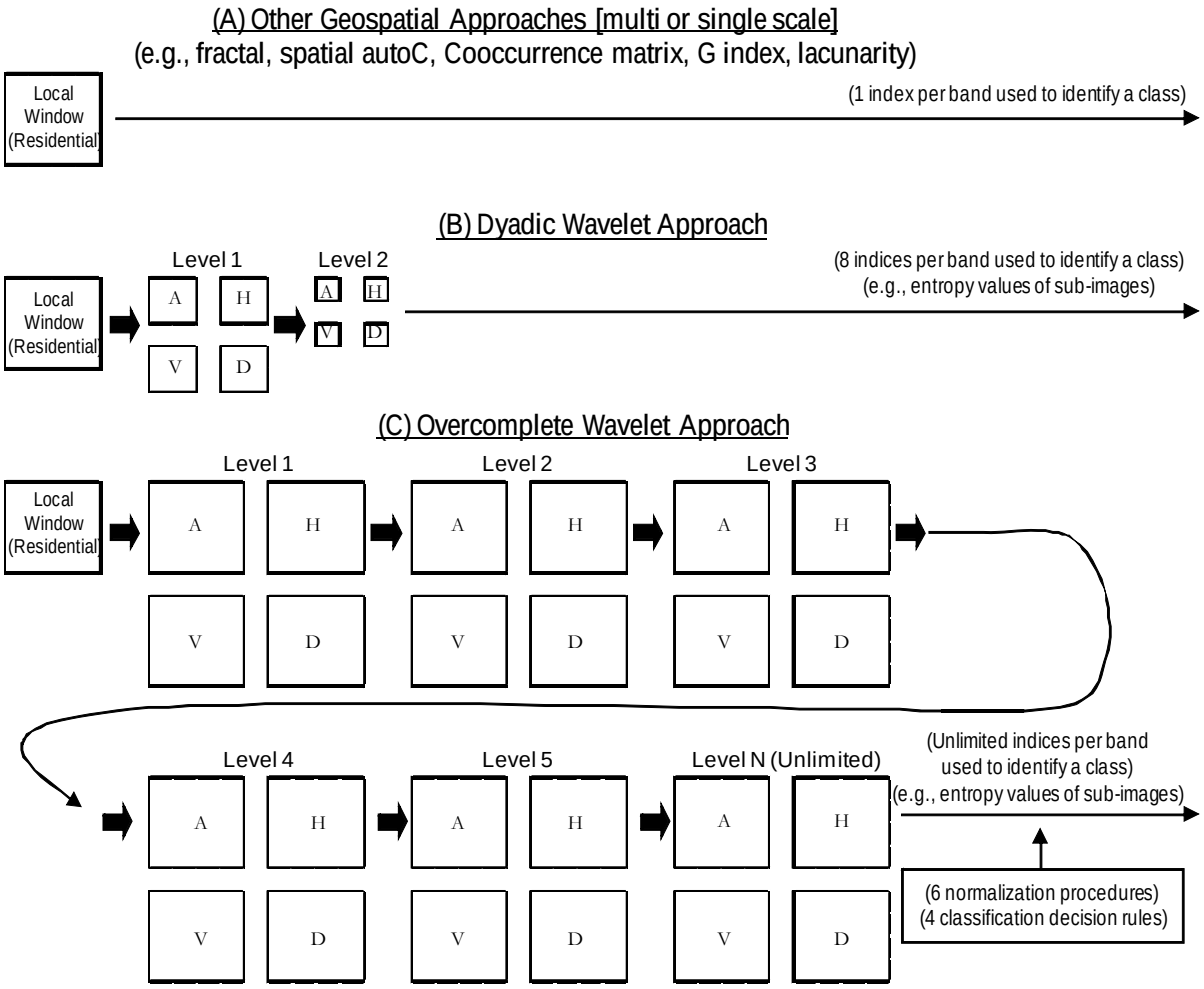

Figure 6. An example of feature vectors or indices (32x32 window or a subset) used to identify an urban class using other geospatial approaches, the dyadic wavelet approach, and the overcomplete wavelet approach,

Note: Sub-images at level two in the dyadic approach reach the suggested minimum dimension (8x8 pixels) since any sub-images smaller than eight pixels may not contain any useful spatial information. A sub-image at a higher level is exactly the same as its original size at the preceding level in the overcomplete approach. It should also be noted that the level of scale with the overcomplete approach is unlimited. A = approximation texture; H = horizontal texture; V = vertical texture; D = diagonal texture.

Table 1. Classification procedures and characteristics of the four main classification groups.

	Per-pixel	**Sub-pixel**	**Object-based**	**Geospatial**
Reflectance Conversion	Not required	Necessary	Not required	Not required
Additional Step Before Training Sample Selection	No	No	Segment image into objects	No
Training Samples	Irregular polygons that cover multiple pixels representing selected land cover classes	Spectra of selected endmembers	Segmented objects that cover multiple pixels representing selected land cover classes	Square windows that cover multiple pixels representing selected land cover classes
Commonly Used Spatial Approaches	GLCM	No	GLCM	Fractal, Geary's C Moran's I, Getis index Fourier transforms, Lacunarity index, Wavelet transforms
Widely Used Classifiers	Maximum Likelihood, Mahalanobis Distance, Minimum Distance, Regression Tree, Neural Network Baysian	Linear Spectral Mixture, Multiple Regression, Regression Tree, Neural Network, Baysian MESMA	Nearest Neighbor	Mahalanobis Distance, Minimum Distance
Primary Input for Classification	Training samples are used to identify land cover classes	Endmember spectra are used to quantify fractions of classes	All pixels in each object identified as one of the training sample classes	All pixels in each window are used to identify one class and the winner class is assigned to the center of the local window
No. of Output Layer	One Layer	Multiple Layers	One Layer	One Layer
Output Structure	One class per pixel	One fraction per pixel per class	One class per pixel	One class per pixel
Accuracy Assessment	Randomly selected pixels for error matrix	Correlation between predicted and reference fractions	Randomly selected pixels for error matrix (or) object-based accuracy assessment	Randomly selected pixels for error matrix

Note: GLCM = Gray Level (or) Spatial Co-occurrence Matrix; MESMA = Multiple endmember spectral mixture analysis.

Table 2. Urban remote sensing classifications with regards to spatial, temporal, and sensor resolutions.

	Urban features	**Urban process**	**Spatial resolution**	**Temporal resolution**	**Sensor resolution**
Micro scale: Individual measurements	Building unit (roofs: flat, pitch) (material: tile, natural/metal, synthetic)	Type and architecture Density	1 m– 5 m	1 year– 5 years	Pan–Vis– NIR
	Vegetation unit (tree, shrub)	Type and health Nature	0.25 m– 5 m	1 year– 5 years	Pan–NIR
	Transport unit (width: road lanes, sidewalk) (material: asphalt, concrete, composite)	Infrastructure Mobility and access	0.25 m– 30 m	1 year– 5 years	Pan–Vis– NIR
Macro scale: Aggregation of imperviousness, greenness, soil and water	Residential neighborhood	Suburbanization Gentrification, poverty, crime, racial segregation, etc.	1 km– 5 km	1 year– 10 years	VIS–NIR– TIR
	Industrial/commercial zone	Land use zoning Storm water flow Heat island effect	1 km– 5 km	1 year– 10 years	VIS–NIR– TIR
	Non built urban	Environmental concerns Beautification Public space	1 km– 5 km	1 year– 10 years	VIS–NIR– TIR
	Urban area	Centrality and sprawl Flow and congestion Sustainability	5 km– 100 km	1 year– 10 years	VIS–NIR– TIR–MIR– Radar

(1) Per-pixel Classifier (Classical Approaches)

(2) Sub-pixel Classifier (Spectral Models)

A group of pixels (object vs. spatial)

Output
One class per pixel

Output
Two or more classes per pixel (fractions)

(3) Object-based Classifier

(e.g., An Object – irregular shape)

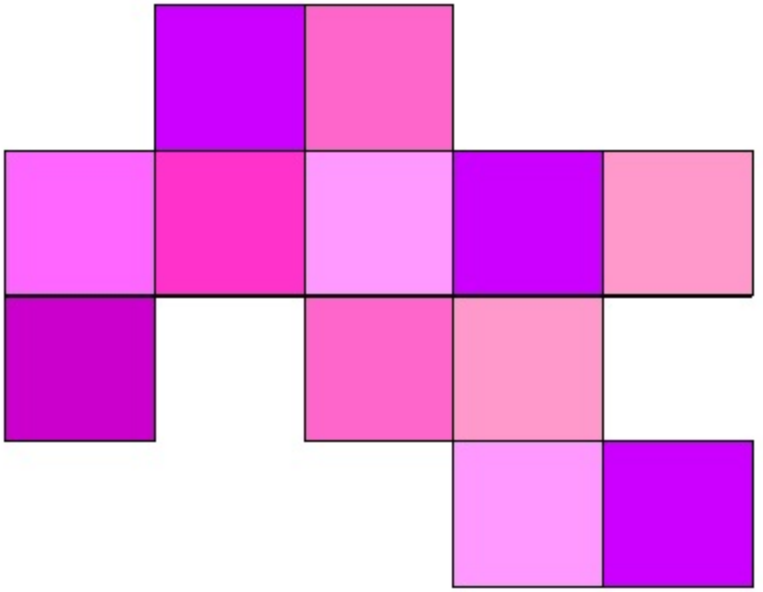

Output = One class per pixel
(All pixels in an object are used to identify a class.
All pixels in an object are identified as a class)

(4) Geospatial Classifier

(e.g., A Local Window – 3x3)

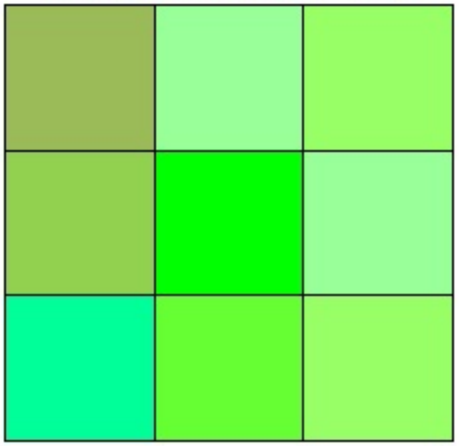

Output = One class per pixel
(All pixels in a window is used to identify a class in the center of the window)

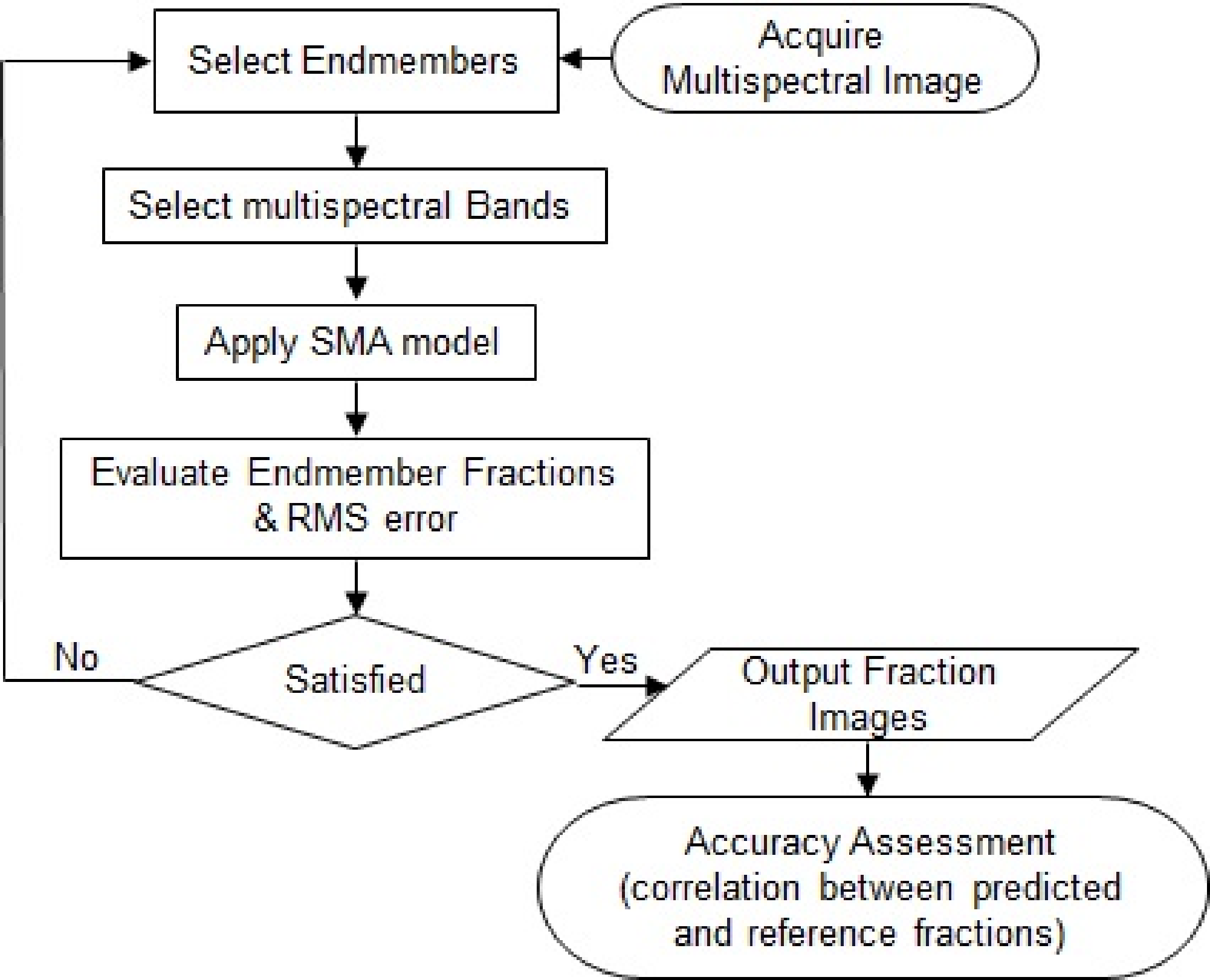
Select Endmembers
Acquire Multispectral Image
Select multispectral Bands
Apply SMA model
Evaluate Endmember Fractions & RMS error
No
Satisfied
Yes
Output Fraction Images
Accuracy Assessment (correlation between predicted and reference fractions)

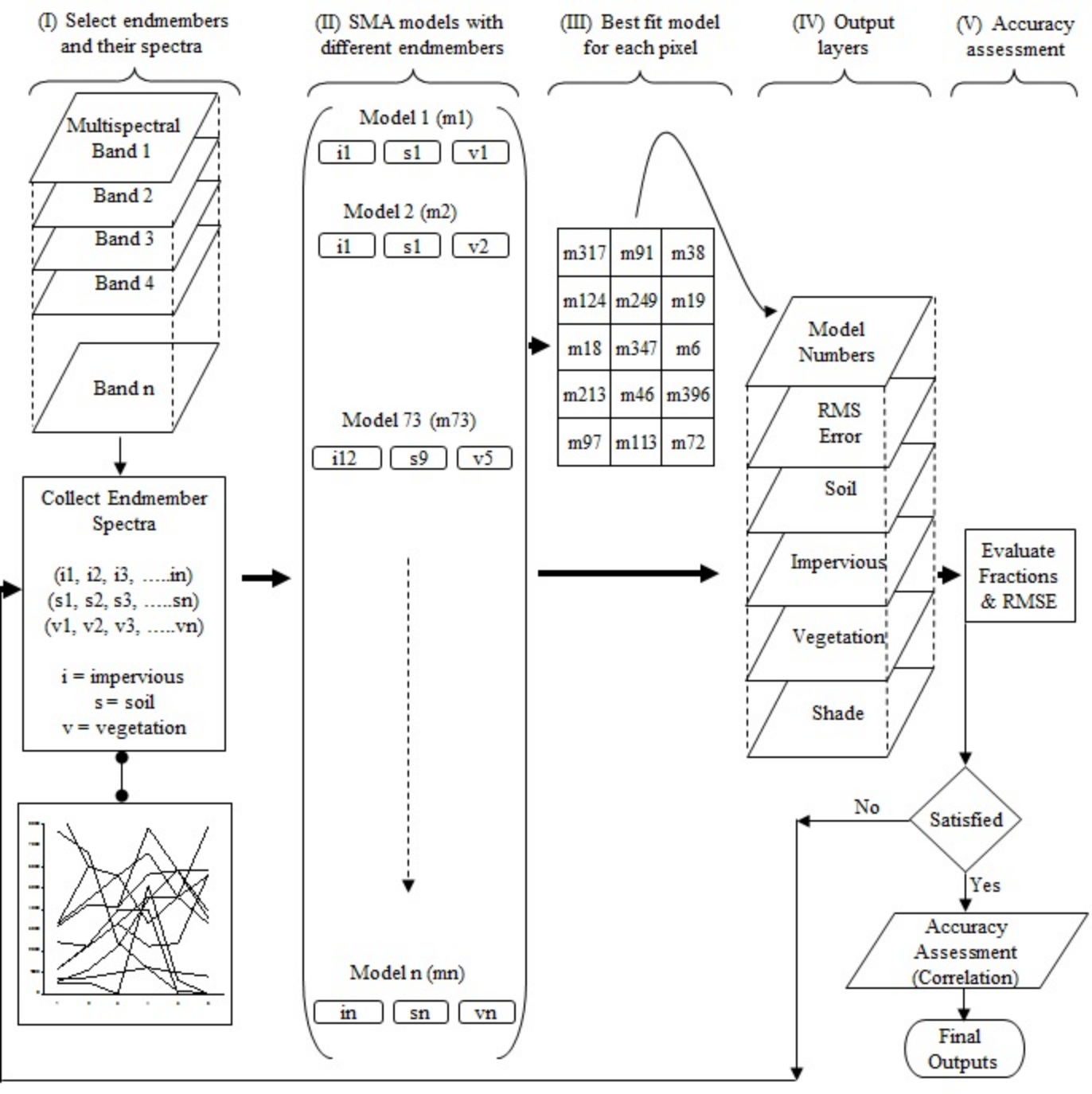
(I) Select endmembers and their spectra
(II) SMA models with different endmembers
(III) Best fit model for each pixel
(IV) Output layers
(V) Accuracy assessment
Multispectral Band 1
Band 2
Band 3
Band 4
Band n
Collect Endmember Spectra
(i1, i2, i3, ...in)
(s1, s2, s3, ...sn)
(v1, v2, v3, ...vn)
i = impervious
s = soil
v = vegetation
Model 1 (m1)
i1 s1 v1
Model 2 (m2)
i1 s1 v2
Model 73 (m73)
i12 s9 v5
Model n (mn)
in sn vn
m317 m91 m38
m124 m249 m19
m18 m347 m6
m213 m46 m396
m97 m113 m72
Model Numbers
RMS Error
Soil
Impervious
Vegetation
Shade
Evaluate Fractions & RMSE
Satisfied
No
Yes
Accuracy Assessment (Correlation)
Final Outputs

(a)

(b)

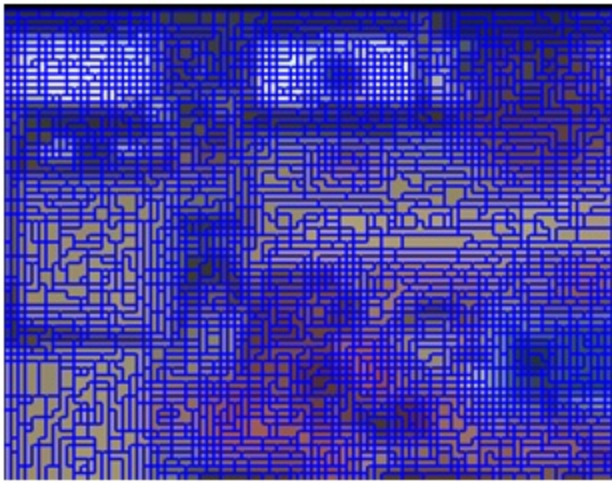

(c)

(d)

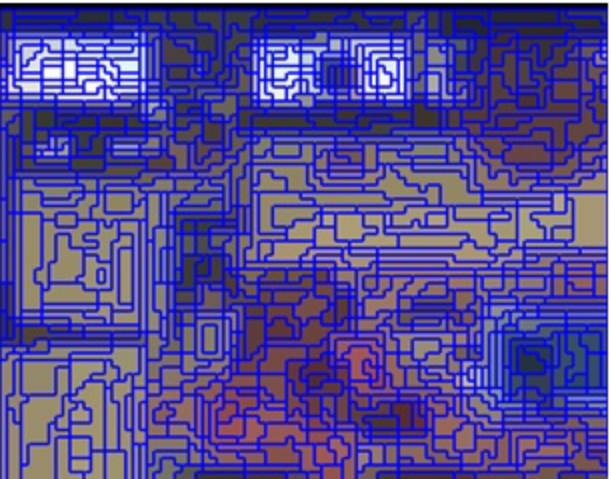

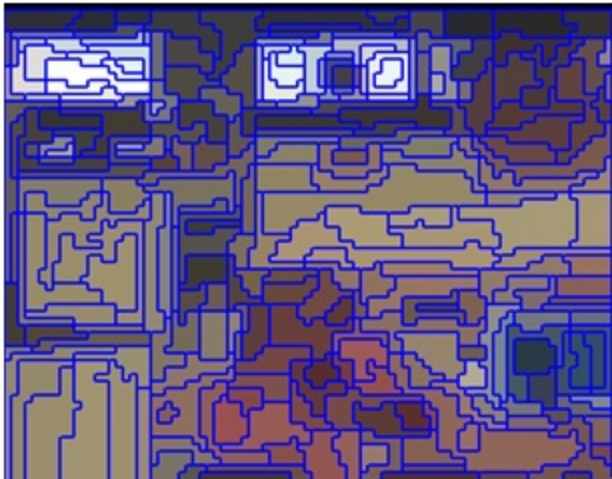

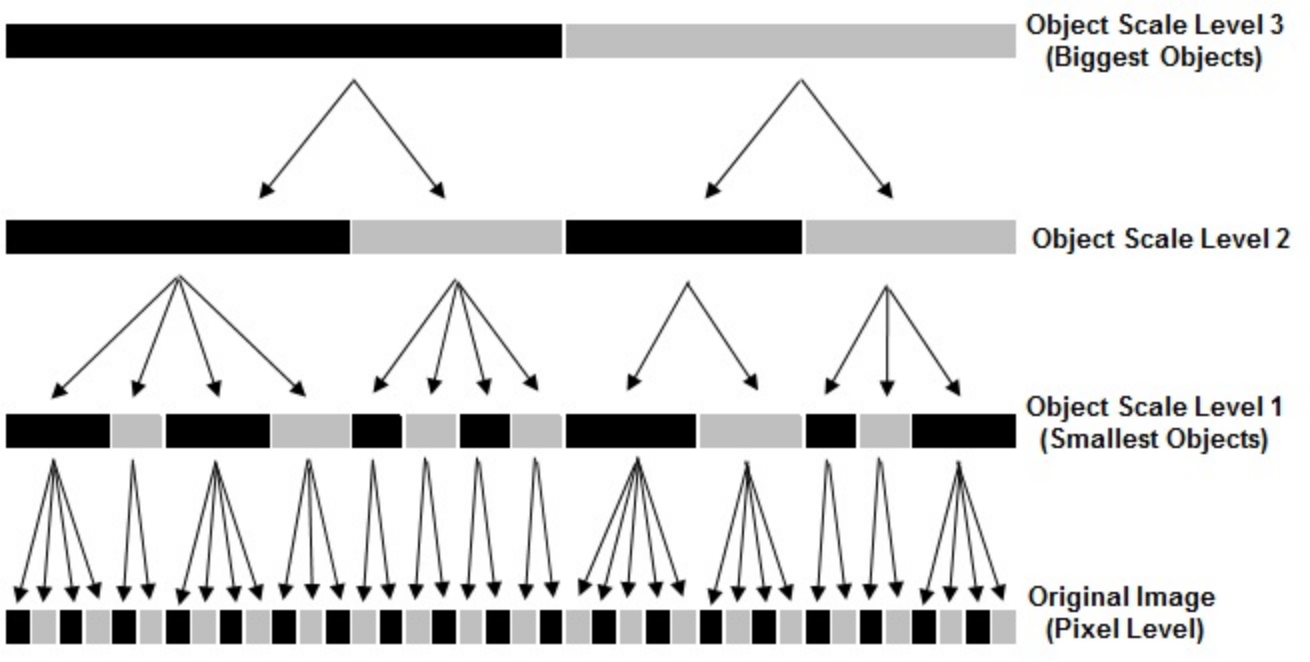
Object Scale Level 3
(Biggest Objects)
Object Scale Level 2
Object Scale Level 1
(Smallest Objects)
Original Image
(Pixel Level)